REGULAR ARTICLE

Change in Energy of Intermolecular Hydrogen Bonds Upon Excitation of Coumarin 120 in Water: A Combined Time-dependent Density Functional Theory / Effective Fragment Potential Study

Mariyappa Ramegowda [a*]

[a] *M Ramegowda, PG Department of Physics, Govt. College (Autonomous), Mandya - 571401, INDIA.*

Abstract: Hydrogen bonding (HB) sites of 7-amino-4-methylcoumarin (C120) in water are investigated theoretically using density functional theory (DFT) interfaced with the effective fragment potential (EFP) method of salvation. The original EFP model (EFP1) is used to form C120-$(H_2O)_7$ complex. Six HBs are formed by C120 with water molecules; one A-type (N···H-O), two B-type (C=O···H-O), two C-type (N-H···O) and one HB (O···H-O) similar to B-type. Excited state properties are computed using time dependent density functional theory (TDDFT) combined with the polarizable continuum model (PCM) and EFP1 method. In S1 state, A type HB energy is increased by 10.18 kJ mol^{-1}, whereas B and C type HB energies are decreased by 6.31 and 11.52 kJ mol^{-1}, respectively.

1.   Introduction

The hydrogen bond interaction in both the ground and excited-states, play a fundamental role in the photochemistry of organic and biological chromophores in solution [1-12].

---

* Corresponding author, *E-mail address*: hmrgowda@yahoo.com (M. Ramegowda)

Several theoretical [13-21] and experimental [22-27] investigations were performed to determine the intermolecular hydrogen bonds, including their structure, energy in the ground state, and energy change upon electronic excitation of molecules. The excited-state HB weakening can heighten the excitation energy of a related excited state and induce an electronic spectral blueshift, whereas the excited-state HB strengthening can lower the excitation energy of a related excited state and induce an electronic spectral redshift [15, 28, 29]. Apart from the influence of the solvent polarity and polarizability, HBs formed between the probes and solvents also influence their structure and photophysical properties [30-34]. The formation of hydrogen bonds can often lead to the appearance of new individuals like S_0-complexes and S_1-exciplexes [35-40].

The EFP method [41-44] provides a polarizable QM-based force field to describe intermolecular interactions. The EFP method embedded with PCM, have been applied successfully to QM/MM studies of molecules in clusters and in solution. The interface of the EFP model with the TDDFT method has been developed for describing electronically excited states of solvated molecules [44-47]. The combined linear response TDDFT (LR-TDDFT) method with the original EFP model (EFP1) was applied successfully to calculate the change in HB energy of aminocoumarins in water [13, 14, 21].

The aminocoumarin molecules represent an important class of organic compounds with extensive and diverse applications [48-51]. They possess distinct biological activity [51] and have been indicated as agents with potential antibiotic, anticancer and anticoagulant activity. They exhibit strong fluorescence in the visible region (from 350 nm to 500 nm), which makes them suitable for use as laser dyes and nonlinear optical chromophores. Aminocoumarins can form one A type HB and two B type HBs due to hydrogen-bond donor properties of electronegative heteroatoms N and O, and two C type HBs via the participation of amino hydrogen atoms with oxygen atom of water molecules [11].

TDDFT/EFP1 calculations have been performed to study the spectral properties and HB dynamics of aminocoumarins [1, 2, 9, 10, 12-14, 21]. The excited-state hydrogen bonding dynamics of aminocoumarin molecules in water have been studied, [12,13,14,21] and demonstrated that A type HB is the strongest in the ground state and it is extremely weakened in an excited state, whereas B and C type HBs are strengthened in the excited state as compared to ground sate. A TDDFT/EFP1 study of hydrogen bonding dynamics of C151 in water shows the formation of additional HB between the oxygen atom of pyrone ring and hydrogen of a water molecule [21].

In the case of C120, there are at least six sites for HB formation with protic solvent molecules as shown in Figure 1; one intermolecular HB N···H-O (type A) is formed by the amino group of C120 with one water molecule, two intermolecular HBs C=O···H-O (type B) are formed by the carbonyl group of C120 with two water molecules, and two HBs of N-

H···O (type C) by hydrogen atoms of the amino group with oxygen atom of water molecules. One HB O···H-O similar to B type is formed between the oxygen atom of the pyrone ring and hydrogen of a water molecule.

In the present work, $C120$-$(H_2O)_7$ complex is formed by using seven EFP1 water molecules with C120 to investigate the possible hydrogen bonding sites of C120 in water. The change in HB energies (ΔE_{HB}'s) of $C120$-$(H_2O)_7$ complex in water as a result of $S_0 \rightarrow S_1$ transition is computed using TDDFT/CPCM/EFP1 method.

2.   Computational methods

All ab initio calculations use the cc-pVDZ basis set [53]. The ground-state and first singlet excited state geometries of $C120$-$(H_2O)_7$ complex were optimized using DFT [54-59] / TDDFT [60-68] with B3LYP [69-71] hybrid functional. Based on optimized ground state geometry, the excitation energies were estimated using TD-CPCM-B3LYP/EFP1/cc-pVDZ method [72, 73, 74]. The DFT based EFP1 water model [43] is used to add explicit water molecules, in which all water molecules are treated as EFPs for DFT and TDDFT calculations. All computations are carried out using the GAMESS-US program package [75, 76].

In $C120$-$(H_2O)_7$ complex, six water molecules formed HB with C120. The HB energy is computed by equating interaction energy between solute and solvent molecules [77]. The optimized geometry of $C120$-$(H_2O)_7$ complex is used to compute the energy of free solute, E_{solu} by removing solvent molecules from the system. Then, the solvent-solute interaction energy can be calculated using the relation,

$$E_{HB} = E_{com} - (E_{solu} + E_{EFP}) \qquad (1)$$

where E_{com} is the total energy of $C120$-$(H_2O)_7$ complex and E_{EFP} is the total effective fragment potential energy. From the optimized geometry of $C120$-$(H_2O)_7$ complex (com7), one water molecule which form a type of HB is removed to calculate the energy of $C120$-$(H_2O)_6$ complex (com6) and energy of the respective type of HB is computed using the equation

$$E_{HB(type)} = (E_{HB})_{com7} - (E_{HB})_{com6} \qquad (2)$$

Then the change in HB energy as a result of $S_0 \rightarrow S_1$ transition is calculated as

$$\Delta E_{HB} = (E_{HB})_{S0} - (E_{HB})_{S1} \qquad (3)$$

3.   Results and discussion

3.1 Geometry and electronic structure at S_0 state

The S_0 state optimized structure of C120-$(H_2O)_7$ complex with atom and HB numbering is shown in **Figure 1**. Six HBs namely, N20···H28-O26 (1.962 Å, type A) O7···H39-O38 (1.832 Å, type B1), O7···H42-O41 (1.855 Å, type B2), O5···H37-O35 (2.066 Å, type B3), N20-H21···O29 (1.831 Å, type C1), N20-H22···O23 (1.949 Å, type C2) are formed by C120 with six water molecules. The calculated bond angles for N20···H28-O26, O7···H39-O38, O7···H42-O41, O5···H37-O35, N20-H21···O29, and N20-H22···O23 are 164.0° 163.3, 162.1, 140.4, 164.9, and 177.2°, respectively. In addition to these six HBs, four inter-water molecular HBs (WHB); O26···H34 (1), O32···H31 (2), O35···H33 (3), and O38···H36 (4) with bond lengths 1.829, 1.672, 1.753 and 1.787 Å, respectively are formed. The optimized parameters of C120 and C120-$(H_2O)_7$ complex at S_0 and S_1 states are presented in **Table 1**.
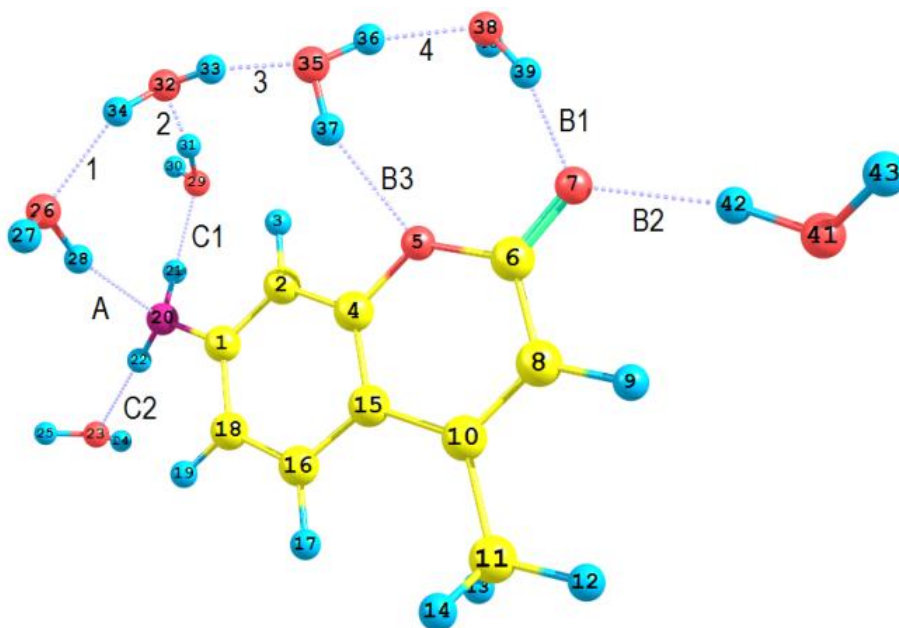

Figure 1: Ground-state optimized structure of C120-$(H_2O)_7$ complex (Red-O, Magenta-N and Yellow-C).

The formation of HBs in C120-$(H_2O)_7$ distorts the electronic structure of C120. In the pyrone ring C4-O5 and C6=O7 bonds are increased by 0.015 and 0.017 Å, whereas O5-C6 and C6-C8 bonds are decreased by 0.019 and 0.011 Å due to B type HBs. The formation of A type and C type HBs causes the increase of C1-N20, N20-H21 and N20-H22 bond lengths by 0.009, 0.011 and 0.005 Å, respectively. Due to complex formation the bond angles of C120 altered by less than 1° except H-N-H angle of the amino group, which changes by 3.2°.

Table 1. Bond lengths, r and bond angles, A of C120 and C120-(H$_2$O)$_7$ complex in S$_0$ and S$_1$ state

r/A	C120		C120-(H$_2$O)$_7$	
(Å/ °)	S$_0$	S$_1$	S$_0$	S$_1$
R(1-2)	1.406	1.416	1.410	1.428
R(1-18)	1.419	1.421	1.423	1.414
R(1-20)	1.370	1.369	1.379	1.363
R(2-4)	1.393	1.390	1.389	1.406
R(4-5)	1.362	1.347	1.377	1.357
R(4-15)	1.415	1.442	1.414	1.403
R(5-6)	1.404	1.458	1.385	1.440
R(6-7)	1.208	1.218	1.225	1.240
R(6-8)	1.453	1.426	1.442	1.423
R(8-10)	1.363	1.404	1.369	1.387
R(10-11)	1.506	1.493	1.505	1.488
R(10-15)	1.449	1.455	1.444	1.491
R(15-16)	1.412	1.422	1.415	1.419
R(16-18)	1.384	1.394	1.383	1.395
R(20-21)	1.009	1.012	1.020	1.023
R(20-22)	1.009	1.012	1.014	1.016
R(20-28)	-	-	1.962	2.278
R(7-39)	-	-	1.832	1.807
R(5-37)	-	-	2.066	1.949
R(7-42)	-	-	1.855	1.826
R(21-29)	-	-	1.831	1.708
R(22-23)	-	-	1.949	1.869
R(26-34)	-	-	1.829	1.836
R(32-31)	-	-	1.672	1.645
R(35-33)	-	-	1.753	1.728
R(38-36)	-	-	1.787	1.806
A(2-1-18)	118.6	119.5	118.4	119.1
A(1-2-4)	120.1	120.6	119.6	120.1
A(1-18-16)	120.4	119.7	120.8	119.0
A(2-4-15)	122.0	121.0	123.1	121.4
A(5-4-15)	121.7	122.7	120.9	123.6
A(4-5-6)	122.2	120.9	122.1	120.4
A(4-15-10)	118.2	118.8	118.4	118.3
A(4-15-16)	116.9	117.2	116.4	117.2
A(5-6-8)	116.1	116.0	117.4	116.5
A(6-8-10)	123.1	125.1	122.1	125.1
A(8-10-15)	118.7	116.5	119.1	116.0
A(15-16-18)	121.9	122.0	121.7	123.0
A(21-20-22)	118.2	117.7	115.0	120.0
A(18-1-20-22)	-000.2	-006.1	-020.7	-005.9
A(2-1-20-21)	-000.8	006.3	024.5	009.1

3.2 Electronic structure at S$_1$ state

In S_1 state the benzene ring of both C120 and C120-(H$_2$O)$_7$ complex, slightly distorted by changing bond lengths ~ 0.01-0.02 Å. The C5-C6 and C6=O7 bonds are elongated, whereas C6-C8 and C10-C11 bonds are contracted. Upon excitation of C120-(H$_2$O)$_7$ complex, C1-N20 and C2-C4 bond lengths changes by -0.016 and 0.017 Å, respectively. The excited state geometry reveals that C8-C10 bond elongated more than C10-C15 bond in C120, whereas in C120-(H$_2$O)$_7$ complex C10-C15 bond elongated more than C8-C10 bond due to strengthening of B type HBs. In S_1 state the variation of bond lengths in pyrone ring causes the slight change in bond angles ~ 2 - 3°. The bond angle H21-N20-H22 changes by 5° due to A and C type HBs. The dihedral angles C18-C1-N20-H22 and C2-C1-N20-H21 changes from -0.2 to -6.1° and –0.8 to 6.3°, respectively due to molecular excitation of C120. On the other hand, $S_0 \rightarrow S_1$ transition of C120-(H$_2$O)$_7$ complex causes the change in dihedral angles from -20.7 to -5.9° and 24.5 to 9.1°, respectively. Thus the structural change of the amino group is due to open-closed umbrella-like motion mechanism.
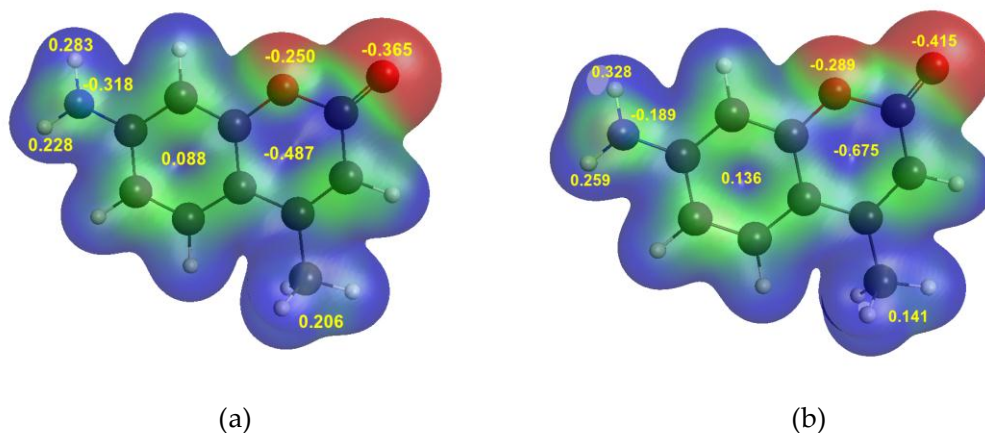

(a)   (b)

Figure 2: Molecular electrostatic potential of C120 at (a) S_0 state and (b) S_1 state with Mulliken charges on various atoms and groups.

The Mulliken charges by the population analysis of C120-(H$_2$O)$_7$ complex have been carried out along with the calculation of HOMO and LUMO. The molecular electrostatic potential (MEP) of C120, and frontier molecular orbitals (MOs) of isolated C120 and C120-(H$_2$O)$_7$ complex are depicted in **Figure 2** and **Figure 3.** From the MEP, it was evident that most electrostatic potential regions (red) were mainly localized over the O5 and O7 atoms, showing the most favorable site for electrophilic attack. Meanwhile, a maximum positive region (blue) is localized on the H atoms, which can be indicating a possible site for nucleophilic attack. The Mulliken charges on O5 and O7 atoms of C120 are -0.250 and -0.365e, respectively. The MEP and Mulliken charges on O5 atom indicating the possibility of

B3 type HB formation. The Mulliken charges on amino, benzene, pyrone (with carbonyl) and methyl groups are 0.193, 0.088,   -0.487 and 0.206e, respectively at S_0 state and 0.398, 0.136 - 0.675 and 0.141e at S_1 state. Upon excitation, the Mulliken charges for N20 atom changes from -0.318 to -0.189e. From **Figure 3** it can also be observed that the intramolecular redistribution of charges from the amino group and benzene ring to pyrone (with carbonyl) and methyl groups of coumarin moiety in both isolated C120 and C120-(H_2O)$_7$ complex. Thus, the S1 state of both isolated C120 and C120-(H_2O)$_7$ complex may be an intramolecular charge-transfer (ICT) state.
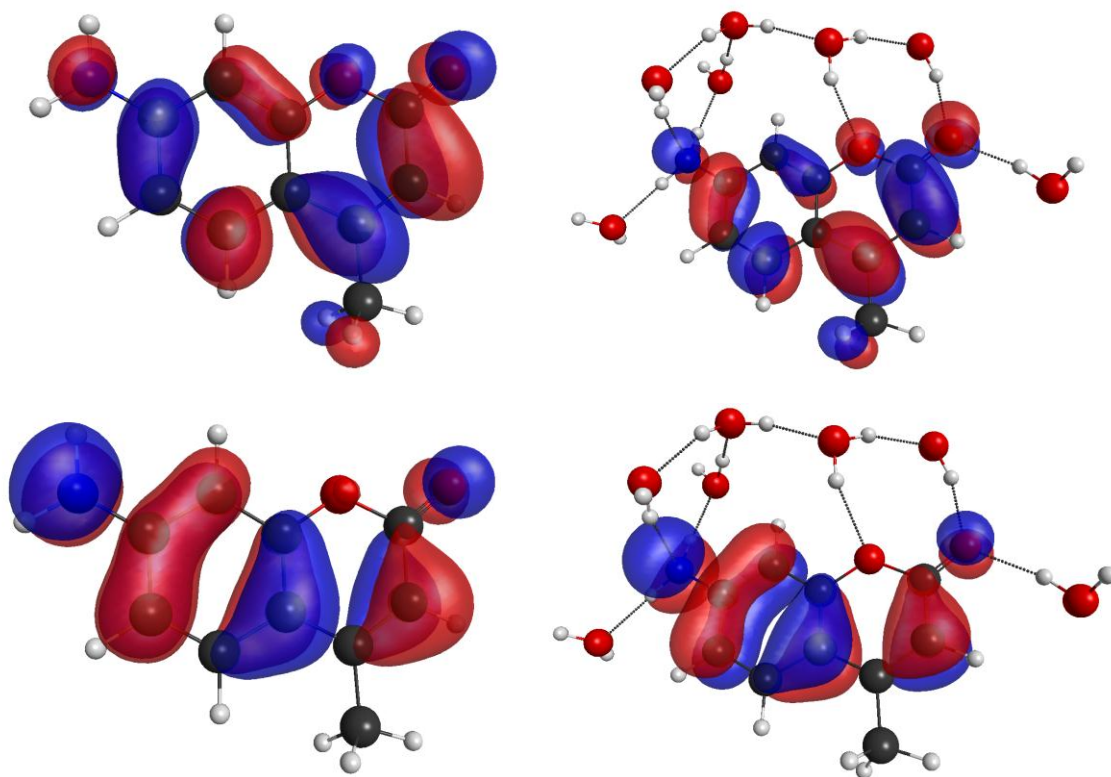

Figure 3: HOMO (bottom) and LUMO (top) of C120 (left) and C120-(H_2O)$_7$ complex (right).

3.3   Electronic spectra and excited state properties

The electronic excitation energies corresponding to $S_0 \rightarrow S_1$ transition and oscillation strengths of C120 and C120-(H_2O)$_7$ complex using the both TDDFT/CPCM and TDDFT/CPCM in combination with salvation model density (SMD) methods are presented in Table 2. SMD uses the solute's quantum mechanical density for PCM electrostatics. It adds corrections for cavitation, dispersion, solvent structure, and also accounts for H-bonding capabilities of solute molecule in solvent medium. The excitation energy of C120 is calculated using the

optimized coordinates of C120-$(H_2O)_7$ by removing EFP molecules. TDDFT/CPCM and TDDFT/CPCM-SMD calculations place the S1 vertical transition for the C120 at 3.768 and 3.737 eV. The decrease in excitation energy using TDDFT/CPCM-SMD method indicates the formation of HBs by C120 in water. C120-$(H_2O)_7$ complex shows the excitation energies at 3.669 and 3.667 eV with TDDFT/CPCM and TDDFT/CPCM-SMD methods respectively. This confirms the formation of six HBs by C120 in water. The calculated values of excitation energies are in consistence with the results obtained by Nguyen et al. [79] (3.640 eV) using PCM-TDB3LYP/ 6- 311++G (d, p) and Zhao et al. [80] (3.646 eV) with PCM–TDB3LYP/ 6-311+G (d, p). However, all these results are in good agreement with the experimental values, 3.625 eV [27,33] and 3.630 [78] within the limit of calculation error (0.010 – 0.039 eV) due to the use of different basis set. In the present work the results deviate from the experimental values by ~ 0.04 eV due to the use of non diffuse basis set.

Table 2. Excitation energy $(S_0 \rightarrow S_1)$, E (eV) and oscillator strength, f of C120 and C120-$(H_2O)_7$ complex.

	TDDFT/CPCM		TDDFT/CPCM-SMD	
	E	f	E	f
C120	3.768	0.585	3.737	0.410
C120-$(H_2O)_7$	3.669	0.389	3.667	0.400

Table 3. Hydrogen bond lengths, r and bond angles, A of C120-$(H_2O)_7$ complex at S_0 and S_1 states.

Type of HB	S_0		S_1	
	r (Å)	A (°)	r (Å)	A (°)
A	1.962	164.0	2.277	148.7
B1	1.832	163.3	1.807	165.0
B2	1.855	162.1	1.826	167.7
B3	2.066	140.4	1.949	147.5
C1	1.831	164.9	1.707	170.3
C2	1.949	177.2	1.869	176.7
WHB1	1.829	-	1.836	-
WHB2	1.672	-	1.645	-
WHB3	1.753	-	1.728	-
WHB4	1.787	-	1.806	-

3.4 Hydrogen bond binding energy

TDDFT calculations of C120-$(H_2O)_7$ complex for the respective type of HB have been carried out by infinitely separating one water molecule, which forms the respective type of HB, and ΔE_{HB}'s are calculated using Equation (2) and (3). **Table 3** lists the HB lengths and angles of C120-$(H_2O)_7$ complex. The A type HB elongated by 0.315 Å, whereas B1, B2, B3, C1 and C2

type HB lengths are contracted by 0.025, 0.029, 0.117, 0.124 and 0.080 Å, respectively. Inter-water molecular HBs; O26···H34, O38···H36 are increased by 0.007, 0.019 Å and O32···H31, O35···H33 are decreased by 0.027, 0.025 Å, respectively.

Table 4 gives the important spectral results of $C120-(H_2O)_7$ complex. As can be seen in **Table 4**, A type HB weakened by 10.18 kJ mol^{-1} energy, whereas B1, B2, B3, C1 and C2 type HB are strengthened by 2.20, 1.74, 2.37, 6.23 and 5.30 kJ mol^{-1}, respectively. The total change in HB energy of $C120-(H_2O)_7$ complex is 6.78 kJ mol^{-1}, which is in perfect agreement with the experimental and estimated data, 6.94 and 7.18 kJ mol^{-1}[27], respectively. The total (sum of all types) change in HB energy is found to be 0.88 kJ mol^{-1} more than the change in HB energy of $C120-(H_2O)_7$ complex. This indicates that the total change in energy of WHBs increases at S_1 state. The scheme applied in this work having the limitation   for the calculation of E_{HB} of individual WHB or only A, B3 and C1 type HBs. The sum of three ΔE_{WHB}'s (1+2+3) is calculated by removing the water molecule H33-O32-H34 form the complex and is found to be 0.83 kJ mol^{-1}. Thus ΔE_{WHB} on the calculation of ΔE_{HB} has lesser effect.

Table 4. Absorption spectral shifts (ΔE), E_{HB} at S_0 and S_1 states, and ΔE_{HB} of $C120-(H_2O)_7$ complex (in kJ mol^{-1})

Type of HB	ΔE	E_{HB} at S_0	E_{HB} at S_1	ΔE_{HB}
A, B, C	-6.75	-414.06	-420.84	6.78
A + 1	10.23	-73.47	-63.29	-10.18
B1 + 4	-2.12	-74.49	-76.69	2.20
B2	-1.74	-53.58	-55.32	1.74
B3 + 1, 4	-2.32	-82.02	-84.39	2.37
C1 + 2	-6.18	-70.61	-76.83	6.22
C2	-5.31	-46.93	-52.23	5.30
1, 2, 3	-0.80	-95.75	-96.58	0.83

The plot of absorption spectral shift, ΔE dependence on ΔE_{HB} for various types of HBs of $C120-(H_2O)_7$ complex relative to C120 monomer is given in **Figure 4**. From this figure, blueshift of spectral lines is observed due to A type HB, whereas redshift of spectral lines is observed due to B1, B2, B3, C1 and C2 type HBs. B1, B2, B3 type HBs shows a nearly equal spectral redshift, and C1, C2 type HBs shows slightly larger redshift. The effect of all A, B and C type HBs in $C120-(H_2O)_7$ complex shows large spectral redshift. This may be the cause of redshift on the absorption spectra of C120 in water imposed by weakening of A type HB and strengthening of B and C type HBs.
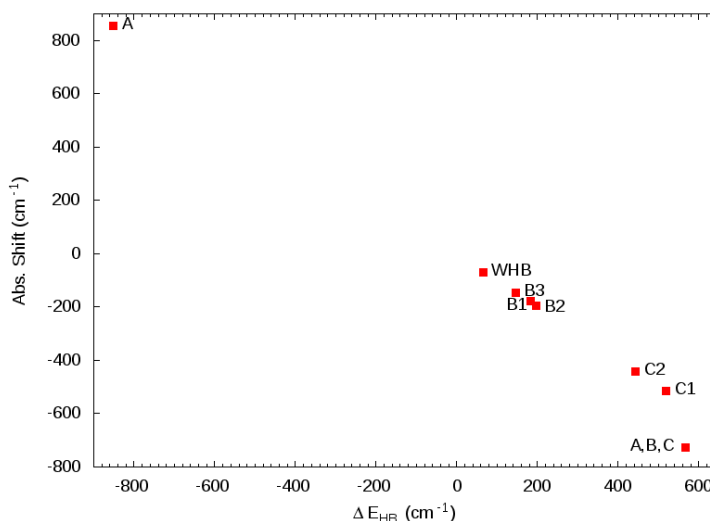
Figure 4: The plot of absorption spectral shift, ΔE dependence on ΔE_{HB} for various types of HBs of C120-$(H_2O)_7$ complex relative to C120 monomer.

From **Table 4**, it can also be noticed that, in S_1 state A type intermolecular HB is weakened due to increase of excitation energy, whereas B type, C type and some of the WHBs are strengthened due to decrease of excitation energy.

4.   Conclusions

In this work, hydrogen bonding sites and electronic excitation energy of solvated C120 have been investigated by means of TD-CPCM-SMD/B3LYP/EFP1/cc-pVDZ methods augmented with explicit inclusion of a seven water molecules, and quantitative agreement between these calculations and literature experimental absorption maxima of C120 in water was obtained with an average error ~ 0.04 eV. C120 molecule formed six HBs with water molecules; one A type, three B type and two C type. As a result of $S_0 \rightarrow S_1$ transition, A type HB weekend by 10.18 kJ mol^{-1}, whereas B1, B2, B3, C1 and C2 type HBs are strengthened by 2.20, 1.74, 2.37, 6.23 and 5.30 kJ mol^{-1}, respectively. In S_1 state, the A type HB length increased by 0.315 Å, whereas B1, B2, B3, C1 and C2 type HB lengths are decreased by 0.025, 0.029, 0.117, 0.124 and 0.080 Å, respectively. In C120-$(H_2O)_7$ complex, four WHBs are formed; upon excitation, two WHBs are elongated and other two are contracted. The quantitative decrease in bond length of WHBs is higher than the increase in bond length of WHBs. This causes the redshift effect on absorption spectra of C120-$(H_2O)_7$ by ~ 0.80 kJ mol^{-1}. In the S_1 state A type intermolecular HB is weakened due to increase of excitation energy, whereas B

type, C type HBs and WHBs are strengthened due to decrease of excitation energy. Therefore, upon excitation, A type HB induces blueshift whereas B and C type HBs induce the redshift.

References

[1] Y. Liu, J. Ding, R. Liu, D. Shi and J. Sun, Revisiting the electronic excited-state hydrogen bonding dynamics of coumarin chromophore in alcohols: Undoubtedly strengthened not cleaved, J. Photochem. Photobiol. A, 201 (2009), 203-207.

[2] P. Zhou, P. Song, J. Liu, K. Han and G. He, Experimental and theoretical study of the rotational reorientation dynamics of 7-animocoumarin derivatives in: hydrogen-bonding effects, Phys. Chem. Chem. Phys., 11 (2009), 9440-9449.

[3] Y. Liu, J. Ding, D. Shi and J. Sun, Time-Dependent Density Functional Theory Study on Electronically Excited States of Coumarin 102 Chromophore in Aniline Solvent: Reconsideration of the Electronic Excited-State Hydrogen-Bonding Dynamics, J. Phys. Chem. A, 112 (2008), 6244-6248.

[4] M. Miao and Y. Shi, Reconsideration on hydrogen bond strengthening or cleavage of photoexcited coumarin 102 in aqueous solvent: A DFT/TDDFT study, J. Comput. Chem., 32 (2011), 3058-3061.

[5] Y. H. Liu and P. Li, Excited-state hydrogen bonding effect on dynamic fluorescence of coumarin 102 chromophore in solution: A time-resolved fluorescence and theoretical study, J. Lumin., 131 (2011), 2116-2120.

[6] E. Pines, D. Pines, Y. Z. Ma and G. R. Fleming, Femtosecond Pump-Probe Measurements of Solvation by Hydrogen-Bonding Interactions, Chem. Phys. Chem., 5 (2004), 1315-1327.

[7] E. T. J. Nibbering, H. Fidder and E. Pines, Ultrafast chemistry: using time-resolved vibrational spectroscopy for interrogation of structural dynamics, Rev. Phys. Chem., 56 (2005), 337-367.

[8] G. J. Zhao and K. L. Han, Hydrogen Bonding in the Electronic Excited State, Acc. Chem. Res., 45 (2012) 404-413.

[9] G. J. Zhao and K. L. Han, Ultrafast Hydrogen Bond Strengthening of the Photoexcited Fluorenone in Alcohols for Facilitating the Fluorescence Quenching, J. Phys. Chem. A, 111 (2007), 9218-9223.

[10] W. Zhao, L. Pan, W. Bian and J. Wang, Influence of Solvent Polarity and Hydrogen Bonding on the Electronic Transition of Coumarin 120: A TDDFT Study, Chem. Phys. Chem., 9 (2008), 1593-1602.

[11] G. J. Zhao, J. Y. Liu, L. C. Zhou and K. L. Han, Site-Selective Photoinduced Electron Transfer from Alcoholic Solvents to the Chromophore Facilitated by Hydrogen Bonding: A New Fluorescence Quenching Mechanism, J. Phys. Chem. B, 111 (2007), 8940-8945.

[12] M. Zhang, B. Ren, Y. Wang and C. Zhao, A DFT/TDDFT study on the excited-state hydrogen bonding dynamics of 6-aminocoumarin in water solution, Spectrochimica Acta Part A, 101 (2013), 191-195.

[13] M. Ramegowda, Change in energy of hydrogen bonds upon excitation of 6-aminocoumarin: TDDFT/EFP1 study, New J. Chem., 37 (2013), 2648-2653.

[14] M. Ramegowda, Change in Energy of Hydrogen Bonds upon Excitation of Coumarin 1: TDDFT/EFP1 Method. Res. J. Chem. Sci., 3(7) (2013), 1-4.

[15] G. J. Zhao and K. L. Han, Effects of Hydrogen Bonding on Tuning Photochemistry: Concerted Hydrogen-Bond Strengthening and Weakening, Chem. Phys. Chem., 9 (2008), 1842-1846.

[16] G. J. Zhao and K. L. Han, Early Time Hydrogen-Bonding Dynamics of Photoexcited Coumarin 102 in Hydrogen-Donating Solvents: Theoretical Study, J. Phys. Chem. A, 111 (2007), 2469-2474.

[17] K. L. Han and G. J. Zhao, Hydrogen Bonding Transfer in the Excited State, John Wiley & Sons Ltd., (2011).

[18] Y. H. Liu and S. C. Lan, Questionable Excited-State H-Atoms Transfer Mechanism for 7-Hydroxyquinoline-(NH3)3 Cluster, Commun. Comput. Chem., 1 (2013), 1-7.

[19] G. Y. Li, Y. H. Li, H. Zhang and G. H. Cui, Time-Dependent Density Functional Theory Study on a Fluorescent Chemosensor Based on C–H···F Hydrogen-Bond Interaction, Commun. Comput. Chem. 1 (2013), 88-98.

[20] G. J. Zhao and K. L. Han, Site-Specific Solvation of the Photoexcited Protochlorophyllide a in Methanol: Formation of the Hydrogen-Bonded Intermediate State Induced by Hydrogen-Bond Strengthening, Biophys. J., 94 (2008), 38-46

[21] M. Ramegowda, A TDDFT/EFP1 study on hydrogen bonding dynamics of coumarin 151 in water, Spectrochimica Acta Part A, 137 (2015), 99–104.

[22] A. Morimoito, T. Yatsuhashi, T. Shimada, L. Biczok, D. A. Tryk and H. Inoue, Radiationless Deactivation of an Intramolecular Charge Transfer Excited State through Hydrogen Bonding: Effect of Molecular Structure and Hard–Soft Anionic Character in the Excited State, J. Phys. Chem. A, 105 (2001), 10488–10496.

[23] L. Biczok, T. Berces and H. Linschitz, Quenching Processes in Hydrogen-Bonded Pairs: Interactions of Excited Fluorenone with Alcohols and Phenols, J. Am. Chem. Soc., 119 (1997), 11071–11077.

[24] V. Vetokhina, M. Kijak, G. Wiosna-Salyga, R. P. Thummel, J. Herbich and J. Waluk, On the origin of fluorescence quenching of pyridylindoles by hydroxylic solvents, Photochem. Photobiol. Sci., 9 (2010) 923-930.

[25] A. Kyrychenko and J. Waluk, Excited-state proton transfer through water bridges and structure of hydrogen-bonded complexes in 1H-pyrrolo[3,2-h]quinoline: adiabatic time-dependent density functional theory study, J. Phys. Chem. A, 110 (2006), 11958-11967.

[26] J. Waluk, Hydrogen-Bonding-Induced Phenomena in Bifunctional Heteroazaaromatics, Acc. Chem. Res., 36 (2003), 832-838.

[27] E. Krystkowiak and A. Maciejewski, Changes in energy of three types of hydrogen bonds upon excitation of aminocoumarins determined from absorption solvatochromic experiments, Phys. Chem. Chem. Phys., 13 (2011), 11317-11324.

[28] H. Wang, M. Wang, E. Liu, M. Xin and C. Yang, DFT/TDDFT study on the excited-state hydrogen bonding dynamics of hydrogen-bonded complex formed by methyl cyanide and methanol, Comput. Theor. Chem., 964 (2011), 243–247.

[29] H. Wang, M. Wang, M. Xin, E. Liu and C. Yang, Excited-state hydrogen bonding dynamics of methyl isocyanide in methanol solvent: A DFT/TDDFT study, Cent. Eur. J. Phys., 9 (2011), 792–799.

[30] G. Jones II, W.R. Jackson and A. M. Halpern, Medium effects on fluorescence quantum yields and lifetimes for coumarin laser dyes, Chem. Phys. Lett., 72 (1980), 391-395.

[31] M. J. Kamlet, C. Dickinson and R. W. Taft, Linear solvation energy relationships Solvent effects on some fluorescence probes, Chem. Phys. Lett., 77 (1981), 69-72.

[32] V. Masilamani and B. M. Sivaram, Solvent effects on the spectral and gain characteristics of a DAMC dye laser, J. Lumin., 27 (1982), 147-154.

[33] T. L. Arbeloa, F. L. Arbeloa, M. J. Tapia and I. L. Arbeloa, Hydrogen-bonding effect on the photophysical properties of 7-aminocoumarin derivatives, J. Phys. Chem., 97 (1993), 4704–4707.

[34] T. L. Arbeloa, F. L. Arbeloa, M. J. Tapia Estevez and I. L. Arbeloa, Binary solvent effects on the absorption and emission of 7-aminocoumarins, J. Lumin., 59 (1994), 369–375.

[35] E. Krystkowiak, K. Dobek and A. Maciejewski, Origin of the strong effect of protic solvents on the emission spectra, quantum yield of fluorescence and fluorescence lifetime of 4-aminophthalimide Role of hydrogen bonds in deactivation of S1-4-aminophthalimide, J. Photochem. Photobiol., A 184 (2006), 250-264.

[36] K. Matsubayashi and Y. Kubo, Control of Photophysical Properties and Photoreactions of Aromatic Imides by Use of Intermolecular Hydrogen Bonding, J. Org. Chem., 73 (2008), 4915–4919.

[37] V. Samant, A. K. Singh, G. Ramakrishna, H. N. Ghosh, T. K. Ghanty and D. K. Palit, Ultrafast Intermolecular Hydrogen Bond Dynamics in the Excited State of Fluorenone, J. Phys. Chem. A, 109 (2005), 8693-8704.

[38] M. A. Munoz, M. Galan, L. Gomez, C. Carmona, P. Guardado and M. Balon, The pyrrole ring as hydrogen-bonding π-donor base: an experimental and theoretical study of the interactions of N-methylpyrrole with alcohols, Chem. Phys., 290 (2003), 69-77.

[39] C. Carmona, M. Balon, M. Galan, P. Guardado and M. A. Munoz, Dynamic Study of Excited State Hydrogen-bonded Complexes of Harmane in Cyclohexane–Toluene Mixtures, Photochem. Photobiol., 76 (2002), 239-246.

[40] C. Carmona, M. Balon, M. Galan, G. Angulo, P. Guardado and M. A. Munoz, Kinetic Study of Hydrogen Bonded Exciplex Formation of N 9 -methyl Harmane, J. Phys. Chem. A, 105 (2001), 10334-10338.

[41] P. N. Day, J. H. Jensen, M. S. Gordon, S. P. Webb, W. J. Stevens, M. Krauss, D. Garmer, H. Basch and D. Cohen, An effective fragment method for modeling solvent effects in quantum mechanical calculations, J. Chem. Phys., 105 (1996), 1968-1986.

[42] M. S. Gordon, M. A. Freitag, P. Bandyopadhyay, J. H. Jensen, V. Kairys and W. J. Stevens, The Effective Fragment Potential Method: A QM-Based MM Approach to Modeling Environmental Effects in Chemistry, J. Phys. Chem., A 105 (2001), 293-307.

[43] I. Adamovic, M. A. Freitag and M. S. Gordon, Density Functional Theory Based Effective Fragment Potential Method, J. Chem. Phys., 118 (2003), 6725-6732.

[44] S. Yoo, F. Zahariev, S. Sok and M. S. Gordon, Solvent effects on optical properties of molecules: A combined time-dependent density functional theory/effective fragment potential approach, J. Chem. Phys., 129 (2008), 144112-8.

[45] D. Si and H. Li, Analytic energy gradient in combined time-dependent density functional theory and polarizable force field calculation, J. Chem. Phys., 133 (2010), 144112-12.

[46] N. Minezawa, N. De Silva, F. Zahariev and M. S. Gordon, Implementation of the analytic energy gradient for the combined time-dependent density functional theory/effective fragment potential method: Application to excited-state molecular dynamics simulations, J. Chem. Phys., 134 (2011), 154111-9.

[47] P. Arora, L. V. Slipchenko, S. P. Webb, A. DeFusco and M. S. Gordon, Solvent Induced frequency shifts: Configuration Interaction Singles combined with the Effective Fragment Potential Method, J. Phys. Chem. A, 114 (2010), 6742–6750.

[48] D. Singer, S. L. Lalama, J. E. Sohn and R. D. Small, Non-linear optical properties of Organic molecules, Crystals, Academic Press, Orlando, F L (1987), ch. II-8.

[49] F. Nicoud and R. J. Twieg, Non-linear optical properties of Organic molecules, Crystals, Academic, Orlando, FL (2002), ch. II-3.

[50] W. E. Moerner and S. M. Silence, Polymeric photorefractive materials, Chem. Rev. 94 (1994), 127-155.

[51] R. O´Kennedy, Coumarins Biology, Applications Mode of Action, Wiley, Chichester, (1997).

[52] T. Gustavsson, T. L. Cassara, V. Gulbinas, G. Gurzadyan, J. C. Mialocq, S. Pommeret, M. Sorgius and P. V. D. Meulen, Femtosecond Spectroscopic Study of Relaxation Processes of Three Amino-Substituted Coumarin Dyes in Methanol and Dimethyl Sulfoxide, J. Phys. Chem. A, 102 (1998), 4229-4245.

[53] T. H. Dunning, Gaussian Basis Sets for Use in Correlated Molecular Calculations. I. The Atoms Boron Through Neon and Hydrogen, J. Chem. Phys., 90 (1989), 1007-1023.

[54] R. G. Parr and W. Yang, Density-Functional Theory of Atoms, Molecules New York: Oxford University Press. (1989).

[55] K. Kim and K. D. Jordan, Comparison of Density Functional and MP2 Calculations on the Water Monomer and Dimer, J. Phy. Chem., 98 (1994), 10089-10094.

[56] P. J. Stephens, F. J. Devlin, C. F. Chabalowski and M. J. Frisch, Ab Initio Calculation of Vibrational Absorption and Circular Dichroism Spectra Using Density Functional Force Fields, J. Phy. Chem., 98 (1994), 11623-11627.

[57] W. H. Stevens, H. Basch, M. Krauss and P. Jasien, Relativistic compact effective potentials and efficient, shared-exponent basis sets for the third-, fourth-, and fifth-row atoms, Can. J. Chem., 70 (1992), 612-630.

[58] T. R. Cundari and W. J. Stevens, Effective core potential methods for the lanthanides, J. Chem. Phys., 98 (1993), 5555-5565.

[59] P. J. Hay and W. R. Wadt, Ab initio effective core potentials for molecular calculations. Potentials for the transition metal atoms Sc to Hg, J. Chem. Phys., 82 (1985), 270-283.

[60] A. Dreuw and M. H. Gordon, Single-Reference ab Initio Methods for the Calculation of Excited States of Large Molecules, Chem. Rev., 105 (2005), 4009-4037.

[61] P. Elliott, F. Furche and K. Burke, Excited states from time-dependent density functional theory, Rev. Comp. Chem., 26 (2009), 91-166.

[62] S. Hirata and M. H. Gordon, Time-dependent density functional theory within the Tamm−Dancoff approximation, Chem. Phy. Lett., 314 (1999), 291-299.

[63] E. Runge and E. K. U. Gross, Density-Functional Theory for Time-Dependent Systems, Phys. ReV. Lett., 52 (1984), 997–1000.

[64] M. Casida, In Recent Advances in Density Functional Methods; D.P. Chong, Ed., World Scientific: Singapore (1995), Vol. 1, pp 155-192.

[65] R. Bauernschmitt and R. Ahlrichs, Treatment of electronic excitations within the adiabatic approximation of time dependent density functional theory, Chem. Phys. Lett., 256 (1996), 454-464.

[66] R. E. Stratmann, G. E. Scuseria and M. J. Frisch, An efficient implementation of time-dependent density-functional theory for the calculation of excitation energies of large molecules, J. Chem. Phys., 109 (1998), 8218-8224.

[67] F. Furche and R. Ahlrichs, Adiabatic time-dependent density functional methods 5. for excited state properties, J. Chem. Phys., 117 (2002), 7433-7477.

[68] F. Furche and R. Ahlrichs, Time-dependent density functional methods for excited state properties, J. Chem. Phys., 121 (2004), 12772-12773.

[69] A. D. Becke, Density-functional thermochemistry. III. The role of exact exchange , J. Chem. Phys., 98 (1993), 5648-5652.

[70] A. D. Becke, Density-functional exchange-energy approximation with correct asymptotic behavior, Phys. ReV. A, 38 (1988), 3098-3100.

[71] C. Lee, W. Yang, and R. G. Parr, Development of the Colle-Salvetti correlation-energy formula into a functional of the electron density, Phys. ReV. B, 37 (1988), 785-789.

[72] H. Li, C. S. Pomelli and J. H. Jensen, Continuum solvation of large molecules described by QM/MM: a semi-iterative implementation of the PCM/EFP interface, Theoret. Chim. Acta, 109 (2003), 71-84.

[73] H. Li, Quantum mechanical/molecular mechanical/continuum style solvation model: linear response theory, variational treatment, and nuclear gradients, J. Chem. Phys., 131 (2009), 184103.

[74] Y. Wang and H. Li, Excited state geometry of photoactive yellow protein chromophore: a combined conductorlike polarizable continuum model and time-dependent density functional study, J. Chem. Phys., 133 (2010), 034108-8.

[75] W. Schmidt, K. K. Baldridge, J. A. Boatz, S. T. Elbert, M. S. Gordon, J. H. Jensen, S. Koseki, N. Matsunaga, K. A. Nguyen, S. J. Su, T. L. Windus, M. Dupuis and J. A. Montgomery, General Atomic and Molecular Electronic Structure System, J. Comp. Chem., 14 (1993), 1347-1363.

[76] M. S. Gordon and M. W. Schmidt, Advances in electronic structure theory: GAMESS a decade later, Chapter 41, pp 1167-1189, in Theory Applications of Computational Chemistry, the first forty years, (Eds,: C. E. Dykstra, G. Frenking, K. S. Kim and G. E. Scuseria), Elsevier, Amsterdam, (2005).

[77] T. Nagata, D. G. Fedorov, T. Sawada, K. Kitaura and M. S. Gordon, A combined effective fragment potential-fragment molecular orbital method. II. Analytic gradient and application to the geometry optimization of solvated tetraglycine and chignolin, J. Chem. Phys., 134 (2011), 034110-12.

[78] H. Pal, S. Nad and M. Kumbhakar, Photophysical Properties of Coumarin-120: Unusual Behavior in Nonpolar Solvents, J. Chem. Phys., 119 (2003), 443-452.

[79] K. A. Nguyen, P. N. Day and R. Pachter, Effects of solvation on one- and two-photon spectra of coumarin derivatives: A time-dependent density functional theory study, J. Chem. Phys., 126 (2007), 094303-10.

[80] W. Zhao, L. Pan, W. Bian and J. Wang, Influence of Solvent Polarity and Hydrogen Bonding on the Electronic Transition of Coumarin 120: A TDDFT Study, Chem. Phys. Chem., 9 (2008), 1593 – 1602.